ACS APPLIED MATERIALS & INTERFACES

Research Article

www.acsami.org

Plasmonic Three-Dimensional Transparent Conductor Based on Al-Doped Zinc Oxide-Coated Nanostructured Glass Using Atomic Layer Deposition

Gary A. Malek,*[,†] Tolga Aytug,[‡] Qingfeng Liu,[†] and Judy Wu*[,†]

[†]Department of Physics and Astronomy, University of Kansas, Lawrence, Kansas 66045, United States

[‡]Oak Ridge National Laboratory, Oak Ridge, Tennessee 37831, United States

ABSTRACT: Transparent nanostructured glass coatings, fabricated on glass substrates, with a unique three-dimensional (3D) architecture were utilized as the foundation for designing plasmonic 3D transparent conductors. Transformation of the nonconducting 3D structure to a conducting porous surface network was accomplished through atomic layer deposition of aluminum-doped zinc oxide (AZO). After AZO growth, gold nanoparticles (AuNPs) were deposited by electron-beam evaporation to enhance light trapping and decrease the overall sheet resistance. Field emission scanning electron microscopy and atomic force microcopy images revealed the highly porous, nanostructured morphology of the AZO-coated glass surface along with the in-plane dimensions of the deposited AuNPs. Sheet resistance measurements conducted on the coated samples verified that the electrical properties of the 3D network are comparable to those of untextured two-dimensional AZO-coated glass substrates. In addition, transmittance measurements of the glass samples coated at various AZO thicknesses showed preservation of the transparent nature of each sample, and the AuNPs demonstrated enhanced light scattering as well as light-trapping capabilities.

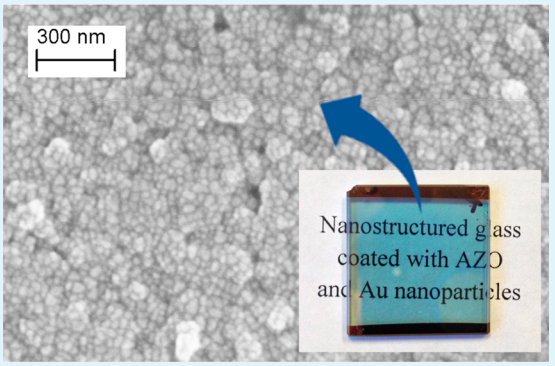

KEYWORDS: *transparent conductor, atomic layer deposition, nanostructured glass, plasmonic effect, three-dimensional electrode, aluminum-doped zinc oxide*

1. INTRODUCTION

Transparent conductors (TCs) are a crucial component of optoelectronic devices that require a conducting surface that is also optically transparent. To date, indium tin oxide (ITO) is the most studied and commonly used transparent conducting oxide (TCO) in various device applications.[1] Despite its high conductivity and transparency, ITO is cost-prohibitive due to the presence of indium. In addition, ITO displays parasitic absorption from 350 to 500 nm, making it less desirable for photovoltaic applications.[2] Therefore, extensive efforts have been dedicated to finding a suitable replacement for ITO.[3,4]

Of particular interest is fabricating TCs into three-dimensional (3D) surface structures that provide a desired enhancement in surface area for various optical, electronic, optoelectronic, and electrochemical applications.[5−8] In general, the majority of device systems employed in such applications have been constructed on glass-based materials. A transparent 3D nanostructured glass template, such as the one developed by Aytug et al., provides a model platform on which a 3D TC can be obtained.[9] The highly porous, nonconducting glass thin film network has a significantly increased surface area (e.g., a factor of 10−100) compared to a planar surface while effectively maintaining the optical transparency of the glass substrate. Therefore, if the highly porous nanostructured glass can be conformally coated with a transparent conducting material, a possible replacement for 3D TCs made from TCOs can be achieved. Unfortunately, due to its highly porous nature, a line-of-sight method provided by well-known physical vapor deposition (PVD) approaches would produce unwanted shadowing effects, and chemical vapor deposition (CVD) would not provide a uniform coating. Hence, the best method to conformally coat 3D surfaces with a high aspect ratio is to use atomic layer deposition (ALD), which employs gas phase precursors that are able to penetrate porous cavities.[10] In our recent work, we successfully coated vertically aligned carbon nanofiber arrays, another example of 3D electrodes with a high aspect ratio of ∼100:1 by ALD to form Al_2O_3 and Al-doped zinc oxide (AZO) core−shell structures.[11] Therefore, a TCO layer deposited by ALD is expected to generate a continuous conducting film throughout the entire porous nanostructured glass surface due to the self-terminating atomic layer growth process. AZO is an excellent choice as a TCO because its conductivity can be controlled by the Zn:Al ratio during the ALD process.[12,13] In addition, the transmittance of AZO extends throughout the entire visible spectrum with a band gap in the range of 3.23 to 3.73 eV depending upon the charge

Received: January 12, 2015
Accepted: April 2, 2015
Published: April 2, 2015

DOI: 10.1021/acsami.5b00336
ACS Appl. Mater. Interfaces 2015, 7, 8556−8561

doping concentration, making it ideal for photovoltaic applications.[14]

Furthermore, the addition of plasmonic metal nanoparticles has been demonstrated as a beneficial approach to improving light management in photovoltaic devices.[15−19] Therefore, plasmonic nanoparticles can be combined with 3D TCO systems to further enhance their light trapping capabilities for improved performance. As light is incident on metal nanoparticles, collective oscillations of electrons on the metal surface are produced. These collective oscillations of electrons, or plasmon, become localized on the metal nanoparticles due to their restricted dimensions. When the frequency of the incident light is resonant with the collective oscillation of the electrons on the surface of the metal nanoparticles, both strong absorption and strong scattering may occur. This resonant frequency is known as localized surface plasmon resonance (LSPR). The complex dielectric constant, dimensions, and shape of the metal nanoparticles, as well as the refractive index of the surrounding material, determine the LSPR frequency. LSPR enhanced light trapping has been demonstrated in our recent study of gold plasmonic nanoparticles self-assembled on 3D fluorine-doped tin oxide (FTO) made with nanoimprint lithography and reactive ion etching.[20] Therefore, gold nanoparticles (AuNPs) can be used in unison with ALD AZO thin films to enhance the performance of a 3D TC for photovoltaic and other optoelectronic applications.

In this article, we explore ALD coating of AZO thin films on porous nanostructured glass in combination with self-assembly of AuNPs atop for utilization as a 3D plasmonic TC (see Figure 1 for a schematic description). This unique plasmonic 3D TC offers a possible replacement for traditional TCs in optoelectronic device applications. In addition, the inherent conductivity of the 3D surface area also merits its utilization for applications that do not require optical transparency (e.g., integrated electrodes for ultracapacitors or other energy storage devices).

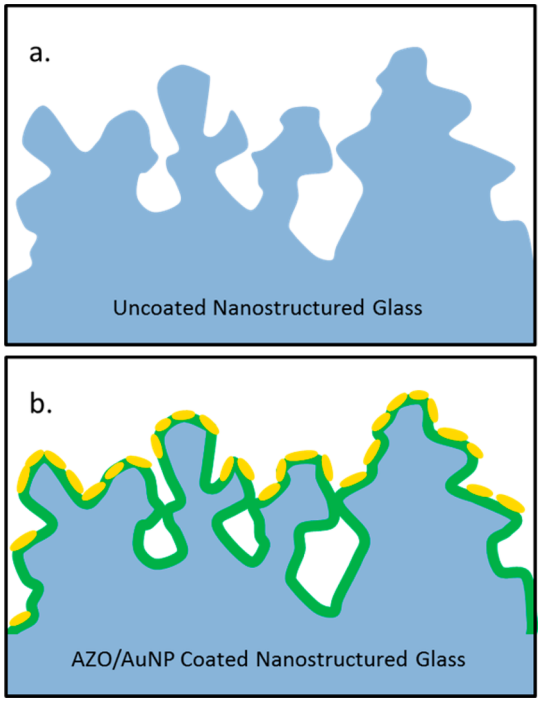

Figure 1. Cross-sectional schematics representing the (a) porous uncoated nanostructured glass (in blue) and (b) coated nanostructured glass with AZO (in green) and AuNPs (in gold).

2. EXPERIMENTAL DETAILS

Radio-frequency magnetron sputtering was used to deposit thin film glass coatings (thickness = 0.5−1 μm) onto fused silica substrates at room temperature using a 2 inch diameter target made from a borosilicate glass composition comprising 66 mol % SiO_2, 26 mol % B_2O_3, and 8 mol % Na_2O. This composition ensures metastable phase separation after postdeposition thermal processing and enables removal of one of the phases through differential etching to create the desired 3D nanoporous surface structure. A detailed description of the nanostructured glass film fabrication has been given in our previous report.[9]

Before the growth of the AZO films, conducting electrodes 21.6 mm apart were applied to the ends of the nanostructured glass for I−V measurements. The electrodes were deposited using electron-beam evaporation and consisted of 8 nm Ti and 50 nm Au. AZO films were then grown in a custom-built ALD system[21] using high-purity H_2O (optima grade, Fisher Scientific), diethylzinc (DEZ, $(C_2H_5)_2Zn$; research grade, SAFC Hitech), and trimethylaluminum (TMA, $Al(CH)_3$; semiconductor grade, Akzo Nobel) as precursors. Ultrahigh purity (UHP, 99.9999%) N_2 was used as the carrier and purging gas with a constant flow rate of 5 sccm throughout all cycles during ALD operation. Every 20 cycles comprised one supercycle where each supercycle contained 19 cycles of alternating H_2O and DEZ for every one doping cycle of H_2O and TMA. The 19:1 Zn/Al doping ratio achieves an AZO resistivity of ~4.2×10^{-3} Ω cm on planar glass. The porous nanostructured glass substrates were heated to 200 °C during AZO growth, and ALD cycling began with H_2O exposure to prepare the nanostructured glass surface with hydroxyl groups for reaction with the first TMA pulse. After each precursor exposure, the ALD chamber and gas feeding lines were purged with UHP N_2 to prevent chemical vapor deposition from occurring. The AZO growth rate is ~0.17 nm/cycle,[11] which is consistent with but slightly less than other published results of ~0.19 nm/cycle with a similar doping ratio.[12−14] Initial AZO growth on the porous nanostructured glass consisted of 5 supercycles (100 total cycles) for an approximate thickness of 17 nm. Subsequent cycles were added to achieve AZO thicknesses of 27, 37, and 47 nm.

After ALD growth of the AZO conducting film, an 8 nm nominal Au film was deposited by electron-beam evaporation, where the thickness of the coating was monitored in situ by a quartz crystal microbalance. The AZO/nanostructured glass substrates were held at 300 °C throughout the Au deposition to facilitate the formation of plasmonic AuNPs.[22]

Surface morphology characterization for the uncoated and coated porous nanostructured glass substrates was accomplished by employing field emission scanning electron microscopy (FESEM, LEO 1550) and atomic force microscopy (AFM, WITec alpha300). Optical transmittance measurements were acquired utilizing a Horiba automated imaging spectrometer (iHR550) with an attached Labsphere integrating sphere (RTC-060-SF). The planar, nonconducting side of the glass was used as the light incident side during the transmittance measurements to represent the typical configuration of a functional solar cell. Electrical characterization was performed on a custom-built, 4-probe system utilizing an Agilent B1505A Power Device Analyzer/Curve Tracer.

3. RESULTS AND DISCUSSION

Figure 1a is a cross-sectional drawing representing the morphology of porous nanostructured glass (blue in color) that is used in this study. Because ALD coating is highly conformal, a continuous AZO film (marked as green) with uniform thickness on top of the nanostructured glass is expected in the selected thickness range as is shown in Figure 2b. Note that with increasing AZO thickness, some of the small pores having radii comparable to the ALD AZO coating thickness may completely close (i.e., the AZO film completely

DOI: 10.1021/acsami.5b00336
ACS Appl. Mater. Interfaces 2015, 7, 8556−8561

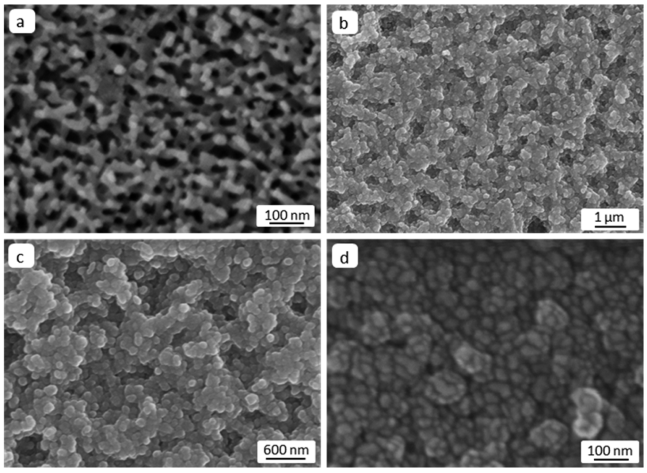

Figure 2. FESEM images of nanostructured glass of (a) uncoated quartz, (b and c) quartz with 47 nm AZO at different magnifications, and (d) borosilicate with 27 nm AZO and 8 nm AuNPs.

fills the openings of some cavities). This results in more of a surface porous nature than a true 3D porous structure, but varying the glass etching conditions as well as utilizing a thinner AZO layer can help prevent this from occurring. Considering the similarities between morphology and surface chemistry, the schematic also shows formation of AuNPs (denoted in gold) on the AZO surface in a fashion similar to those formed on a trapezoidal FTO surface pattern as reported by Wang et al.[20] The trapezoidal FTO surface contained 50 nm diameter AuNPs after deposition of a 15 nm nominal thickness Au film. A finite-difference time-domain simulation of the AuNP/nanopatterned FTO structure revealed that the combination of the photonic structured TCO with plasmonic AuNPs led to a considerable enhancement in light trapping compared to the case of either a photonic or plasmonic nanostructure. Compared to the AuNP/nanopatterned FTO, the AuNP/AZO/porous nanostructured glass reported here has an economical advantage owing to a simplified processing scheme and its scalability for commercialization.

FESEM images taken of the porous nanostructured glass before and after coating with AZO and AuNPs are compared in Figure 2. Figure 2a reveals the coral-like nature of a representative uncoated porous nanostructured glass with approximate pore sizes of 40−80 nm. A substantial difference in surface morphology is apparent after coating with 47 nm AZO, as shown in Figures 2b and c. The rough surface of the nanostructured glass is clearly evident, but it does not appear to be as porous as the uncoated sample. This is to be expected because all of the pores with openings less than twice the deposition thickness will ultimately close. Therefore, if maximum surface area is desired for applications, then it is important to keep the AZO layer as thin as possible while still maintaining the best possible conductivity. However, note that the dimensions of the porosity, as well as the size of the silica skeleton, can easily be manipulated through adjustment of the processing parameters for desired TCO coverage and electrical properties. The ALD-coated AZO has a much smoother surface morphology compared to TCO films constructed from other physical or chemical vapor deposition approaches. For example, commercial FTO films have a distinctive granular surface morphology with feature dimensions typically on the order of a few hundred nanometers.[20] In contrast, the AZO films shown in Figures 2b and c appear to coat the porous glass smoothly and conformally. This is expected because of the layer-by-layer coating mechanism inherent to the ALD process, and the employment of a low growth temperature further prevents mobility of the surface species to form distinctive features. Figure 2d reveals the size and distribution of AuNPs on the surface of nanostructured borosilicate glass coated with 27 nm AZO. For 8 nm Au electron beam deposition at 300 °C, the observed lateral dimensions of the AuNPs between 20 and 50 nm are reasonable according to previously published results.[20,22]

For the surface morphology to be investigated further, AFM was used to compare the porous nanostructured glass before coating with AZO (Figure 3a) to the surface porous nature that appears after coating with AZO and AuNPs (Figure 3b). It can be seen that the roughness of the porous nanostructured glass

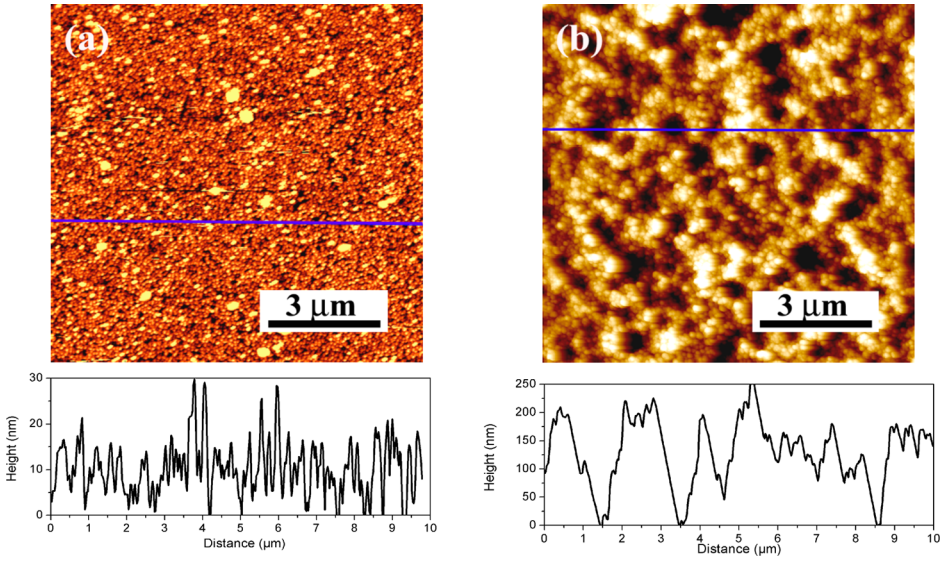

Figure 3. AFM images of the (a) uncoated nanostructured glass and (b) nanostructured glass coated with 47 nm AZO and 8 nm AuNPs. The height profiles were taken along the blue line shown on the AFM images. These profiles reveal the rough nature of the substrate surfaces.

DOI: 10.1021/acsami.5b00336
ACS Appl. Mater. Interfaces 2015, 7, 8556−8561

surface sharply increased after coating a layer of AZO with AuNPs in which the peak-to-valley distance is on the order of 250 nm within the spatial range of only 30 nm. The AuNPs do not show up clearly on the line scan of Figure 3b because their nominal thickness and spacing is very small compared to the peak-to-valley distances shown. The smaller roughness observed on the uncoated sample is most likely caused by inaccessibility of the AFM tip into the small pores of the nanostructured film matrix. In the line scan of Figure 3a, pores are shown as shallow dents of depth on the order of tens of nanometers and appear to occur more frequently than the vertical changes in direction for the line scan of Figure 3b. The overall vertical roughness was brought up after AZO/AuNP coating because the edges around the pores have added height. The increased nonuniformity of the surface roughness may also be attributed to pore size variation. Although larger pores remain, smaller ones might have been completely filled with AZO. It is interesting to note that, comparing the line-scan in Figure 3b with the photonic structures made on FTO using nanoimprint lithography, a comparable lateral pitch size of ~300−500 nm is observable for the AZO-coated porous nanostructured glass as well. In particular, the conversion from the porous to protruding nanostructured surface after ALD AZO coating is beneficial for further fabrication of functional structures atop, such as solar cells, using PVD or CVD methods.

A photograph showing the transparency through an uncoated nanostructured glass sample (on the left) as well as a coated counterpart having 27 nm AZO (on the right) is shown in Figure 4a. The University of Kansas Jayhawk logo is clearly visible through both samples with the coated sample having 89.2% transmittance of the uncoated sample at 550 nm. The sample on the right also shows the Ti/Au contacts that were applied to decrease the contact resistance for electrical measurements. The wavelength-dependent optical transmittance over a spectral range of 400 to 800 nm for 17, 27, 37, and 47 nm thicknesses of AZO films, as well as for the 47 nm AZO coupled with 8 nm AuNP sample, are shown in Figure 4b. As expected, the transmittance decreases with increasing AZO thickness but still stays above 80.5% at 550 nm for the thickest film, which is comparable to that of TCOs employed in solar cells. Once the AuNPs were added to the 47 nm AZO film, the overall transmittance greatly decreased due to plasmonic light trapping associated with the surface AuNPs. This verification of the plasmonic effect is associated with a conversion of the far field light to evanescent light, which cannot be detected by the integrating sphere. These results were anticipated due to the work of Xu et al. who demonstrated the light trapping nature of plasmonic nanoparticles in a simulation of the intensity distribution for the electric field after scattering.[23] The LSPR wavelength λ_P and the minimum transmittance at λ_P were determined to be 728 nm and 25.7%, respectively. In addition to the expected low transmittance, the LSPR wavelength was anticipated to be quite long compared to those determined by Lu et al. for 8 nm AuNPs on SiO_2. Their results produced an LSPR wavelength of 632 nm but, with the addition of a conducting graphene layer between the AuNPs and SiO_2, the LSPR wavelength was red-shifted to 666 nm.[22] Therefore, it is possible that coating the nanostructured glass with a conducting AZO layer was responsible for producing the long LSPR wavelength of 728 nm for the 8 nm AuNPs achieved in this work.

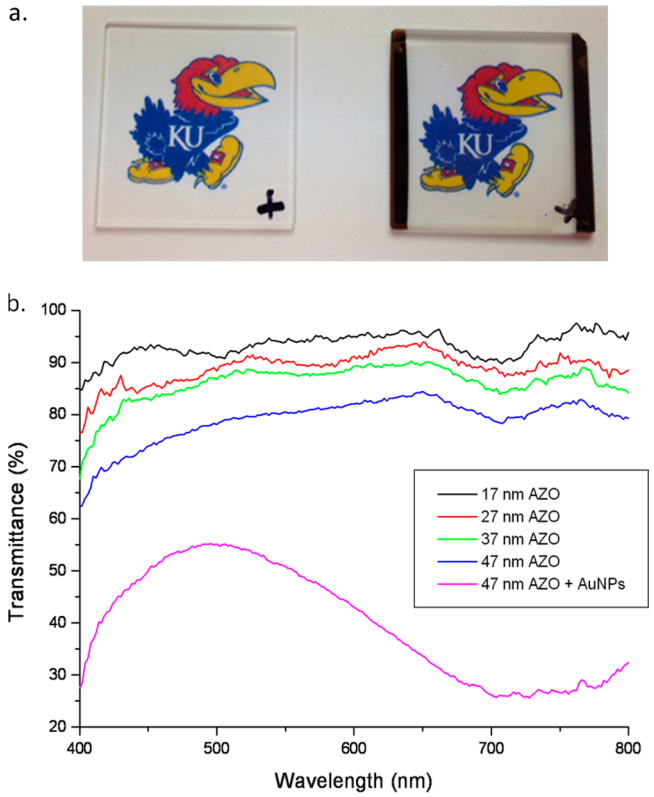

Figure 4. (a) Photograph showing transparency of uncoated nanostructured glass on the left and nanostructured glass with 27 nm AZO coating on the right. (b) Transmittance vs wavelength spectra for the 17, 27, 37, and 47 nm thick AZO coatings. Data for the 47 nm AZO sample with 8 nm AuNPs is also shown, clearly revealing the LSPR wavelength of 728 nm and the corresponding minimum transmittance of 25.7%.

Resistance values of the samples were determined from the I−V curves shown in Figure 5. A clear decreasing trend of 586, 188, 131, 126, and 116 Ω was obtained corresponding to AZO film thicknesses of 17, 27, 37, 47 nm, and 47 nm/AuNPs, respectively. The average length between the Ti/Au contacts was 21.6 mm, and the average width of the nanostructured glass

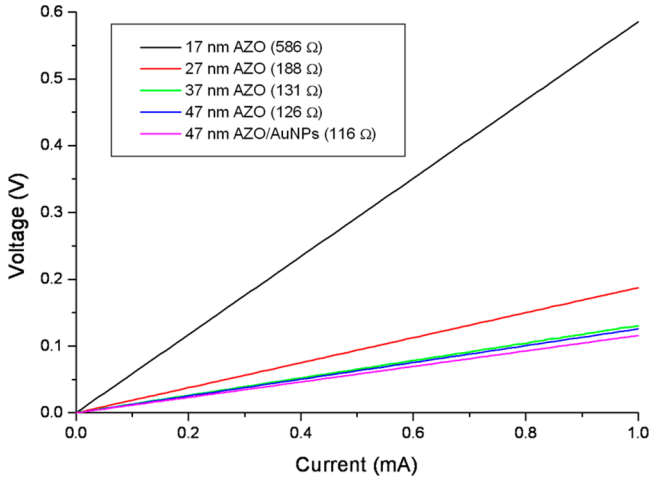

Figure 5. Voltage vs current curves displaying the ohmic nature of the transparent conductors deposited on nanotextured glass substrates. Resistance values obtained for each sample are displayed in the figure.

DOI: 10.1021/acsami.5b00336
ACS Appl. Mater. Interfaces 2015, 7, 8556−8561

was 25.5 mm. These dimensions, along with the resistance values listed above, were utilized to calculate sheet resistance values of 692, 222, 155, 149, and 137 Ω/□, respectively. The greatest decrease in sheet resistance is attained when the thickness of the AZO film reached a critical level >17 nm, above which there is still a steady decline in values, but the relative drop rate is weakened. This can be attributed to the pores with small lateral openings being completely filled with the AZO films having thickness values around 20 nm, providing a completely percolative path for the current transport. Therefore, increased thickness beyond a critical value will not provide as much decrease in sheet resistance. For instance, pores with diameters <74 nm (see Figure 2a) are most likely completely filled when the thickness of the AZO is grown to 37 nm. The corresponding resistivity values of the samples (with only AZO) appear to corroborate this observation. In general, resistivity values should stay constant regardless of the thickness of the conducting film as long as it is not thick enough to be considered a bulk material. The calculated resistivity values are 1.2×10^{-3}, 6.0×10^{-4}, 5.7×10^{-4}, and 7.0×10^{-4} Ω cm for the 17, 27, 37, and 47 nm AZO films, respectively. All of these values are smaller than the 4.2×10^{-3} Ω cm resistivity that our system routinely produces on planar glass substrates; however, after the 27 nm AZO growth, the resistivities obtained on the nanostructured glass appear to trend toward the expected value of counterpart AZO on flat glass.

Figure 6 displays the transmittance values at 550 nm versus their corresponding sheet resistance values for the coated porous nanostructured glass samples. Transmittances of 93.3, 89.2, 88.0, 80.5, and 50.8% were obtained for the AZO thicknesses of 17, 27, 37, 47 nm, and 47 nm/AuNPs, respectively. These values reveal a clear drop in transmittance after the 37 nm thick AZO deposition with very little gain in conductivity. Nevertheless, AZO thicknesses <47 nm still provide optimal light transmittance at >80% while the sheet resistance remains close to or below 150 Ω/□. The optimal combination is observed for the 37 nm thick AZO film with a transmittance of 88.0% and corresponding sheet resistance of 155 Ω/□. These observations are remarkable considering standard commercial TCOs containing ITO or FTO have thicknesses up to hundreds of nanometers, which merits the applicability of TCO-coated porous nanostructured glass for various optoelectronic applications.

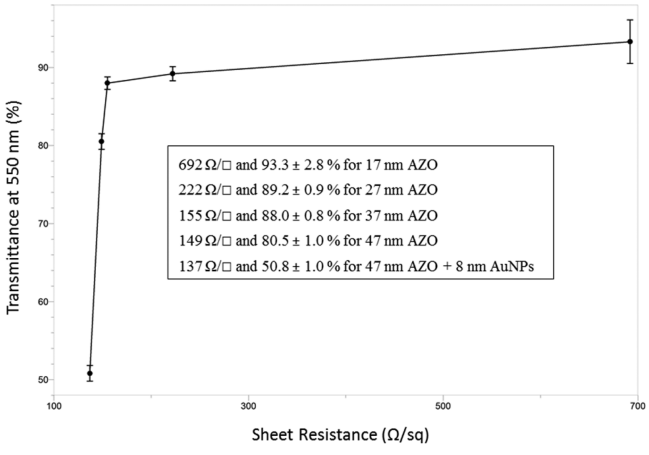

Figure 6. Transmittance at 550 nm vs sheet resistance for different thicknesses of AZO films and AuNPs deposited on the nanostructured glass substrates. The transmittance error bars represent one standard deviation, and the sheet resistance error bars are not shown due to negligible size.

4. CONCLUSIONS

Transparent, nanostructured porous glass film coatings on glass platforms were utilized as a substrate for the fabrication of plasmonic 3D TCs. The nonconducting, porous nanostructured surface was converted to a conducting surface by growing conformal AZO films within the cavities of the glass-film network using ALD. AZO films ranging from 17 to 47 nm were achieved. After ALD AZO growth, AuNPs were incorporated onto the surface of the AZO film to create a plasmonic effect for the 3D TC architecture. FESEM images revealed that the highly porous nature of the conducting nanostructured glass was maintained after AZO and AuNP growth. Line scans from AFM images displayed a large increase in surface roughness after AZO/AuNP coating. Sheet resistance values of ∼150 Ω/□ were obtained for the 37 and 47 nm thick AZO-coated samples with good transmittance properties above ∼80% within the visible regime. The optimal combination of transmittance (88.0% at 550 nm) and sheet resistance (155 Ω/□) was obtained for 37 nm thick AZO films. With the incorporation of AuNPs on the AZO layer, the sheet resistance values were maintained at high quality, and the transmittance decreased significantly due to the plasmonic resonance associated with the AuNPs, providing an LSPR wavelength of 728 nm and a corresponding minimum transmittance of 25.7%. The encouraging results of the plasmonic 3D TC based on AZO-coated nanostructured glass lead to a possible replacement for traditional TCs in optoelectronic device applications. Furthermore, the unique 3D conducting platform may be utilized for devices that do not require optical transparency, such as integrated electrodes for ultracapacitors or other energy storage devices.

AUTHOR INFORMATION

Corresponding Authors

*E-mail: gmalek@ku.edu.

*E-mail: jwu@ku.edu.

Notes

The authors declare no competing financial interest.

ACKNOWLEDGMENTS

The authors acknowledge support in part by NASA contract no. NNX13AD42A, ARO contract no. W911NF-12-1-0412, and NSF contracts nos. NSF-DMR-1105986 and NSF-EPSCoR-0903806, and matching support from the state of Kansas through the Kansas Technology Enterprise Corporation. The nanostructured glass sample preparation conducted at Oak Ridge National Laboratory (ORNL) was supported by the Laboratory Directed Research and Development Program of ORNL, managed by UT-Battelle, LLC for the U.S. Department of Energy.

REFERENCES

(1) Edwards, P. P.; Porch, A.; Jones, M. O.; Morgan, D. V.; Perks, R. M. Basic Materials Physics of Transparent Conducting Oxides. *Dalton Trans.* **2004**, 2995−3002.

(2) Ferry, V. E.; Polman, A.; Atwater, H. A. Modeling Light Trapping in Nanostructured Solar Cells. *ACS Nano* **2011**, *5*, 10055−10064.

(3) Kumar, A.; Zhou, C. W. The Race To Replace Tin-Doped Indium Oxide: Which Material Will Win? *ACS Nano* **2010**, *4*, 11−14.

DOI: 10.1021/acsami.5b00336
ACS Appl. Mater. Interfaces 2015, 7, 8556−8561

(4) Hecht, D. S.; Hu, L. B.; Irvin, G. Emerging Transparent Electrodes Based on Thin Films of Carbon Nanotubes, Graphene, and Metallic Nanostructures. *Adv. Mater.* **2011**, *23*, 1482−1513.
(5) Wang, F.; Subbaiyan, N. K.; Wang, Q.; Rochford, C.; Xu, G.; Lu, R.; Elliot, A.; D'Souza, F.; Hui, R.; Wu, J. Development of Nanopatterned Fluorine-Doped Tin Oxide Electrodes for Dye-Sensitized Solar Cells with Improved Light Trapping. *ACS Appl. Mater. Interfaces* **2012**, *4*, 1565−1572.
(6) Tetreault, N.; Arsenault, E.; Heiniger, L. P.; Soheilnia, N.; Brillet, J.; Moehl, T.; Zakeeruddin, S.; Ozin, G. A.; Gratzel, M. High-Efficiency Dye-Sensitized Solar Cell with Three-Dimensional Photoanode. *Nano Lett.* **2011**, *11*, 4579−4584.
(7) Yang, Z.; Gao, S.; Li, W.; Vlasko-Vlasov, V.; Welp, U.; Kwok, W. K.; Xu, T. Three-Dimensional Photonic Crystal Fluorinated Tin Oxide (FTO) Electrodes: Synthesis and Optical and Electrical Properties. *ACS Appl. Mater. Interfaces* **2011**, *3*, 1101−1108.
(8) Forman, A. J.; Chen, Z.; Chakthranont, P.; Jaramillo, T. F. High Surface Area Transparent Conducting Oxide Electrodes with a Customizable Device Architecture. *Chem. Mater.* **2014**, *26*, 958−964.
(9) Aytug, T.; Simpson, J. T.; Lupini, A. R.; Trejo, R. M.; Jellison, G. E.; Ivanov, I. N.; Pennycook, S. J.; Hillesheim, D. A.; Winter, K. O.; Christen, D. K.; Hunter, S. R.; Haynes, J. A. Optically Transparent, Mechanically Durable, Nanostructured Superhydrophobic Surfaces Enabled by Spinodally Phase-Separated Glass Thin Films. *Nanotechnology* **2013**, *24*, 315602.
(10) George, S. M. Atomic Layer Deposition: An Overview. *Chem. Rev.* **2010**, *110*, 111−31.
(11) Malek, G. A.; Brown, E.; Klankowski, S. A.; Liu, J.; Elliot, A. J.; Lu, R.; Li, J.; Wu, J. Atomic Layer Deposition of Al-Doped ZnO/Al_2O_3 Double Layers on Vertically Aligned Carbon Nanofiber Arrays. *ACS Appl. Mater. Interfaces* **2014**, *6*, 6865−6871.
(12) Hou, Q. Q.; Meng, F. J.; Sun, J. M. Electrical and Optical Properties of Al-Doped ZnO and $ZnAl_2O_4$ Films Prepared by Atomic Layer Deposition. *Nanoscale Res. Lett.* **2013**, *8*.
(13) Elam, J. W.; Sechrist, Z. A.; George, S. M. ZnO/Al_2O_3 Nanolaminates Fabricated by Atomic Layer Deposition: Growth and Surface Roughness Measurements. *Thin Solid Films* **2002**, *414*, 43−55.
(14) Banerjee, P.; Lee, W. J.; Bae, K. R.; Lee, S. B.; Rubloff, G. W. Structural, Electrical, and Optical Properties of Atomic Layer Deposition Al-doped ZnO films. *J. Appl. Phys.* **2010**, *108*, 043504.
(15) Atwater, H. A.; Polman, A. Plasmonics for Improved Photovoltaic Devices. *Nat. Mater.* **2010**, *9*, 205−213.
(16) Ferry, V. E.; Munday, J. N.; Atwater, H. A. Design Considerations for Plasmonic Photovoltaics. *Adv. Mater.* **2010**, *22*, 4794−4808.
(17) Catchpole, K. R.; Polman, A. Plasmonic Solar Cells. *Opt. Express* **2008**, *16*, 21793−21800.
(18) Catchpole, K. R.; Polman, A. Design Principles for Particle Plasmon Enhanced Solar Cells. *Appl. Phys. Lett.* **2008**, *93*, 191113.
(19) Wu, J. L.; Chen, F. C.; Hsiao, Y. S.; Chien, F. C.; Chen, P. L.; Kuo, C. H.; Huang, M. H.; Hsu, C. S. Surface Plasmonic Effects of Metallic Nanoparticles on the Performance of Polymer Bulk Heterojunction Solar Cells. *ACS Nano* **2011**, *5*, 959−967.
(20) Wang, F.; Wang, Q.; Xu, G.; Hui, R.; Wu, J. Light Trapping on Plasmonic-Photonic Nanostructured Fluorine-Doped Tin Oxide. *J. Phys. Chem. C* **2013**, *117*, 11725−11730.
(21) Elliot, A. J.; Malek, G. A.; Lu, R.; Han, S.; Yu, H.; Zhao, S.; Wu, J. Z. Integrating Atomic Layer Deposition and Ultra-High Vacuum Physical Vapor Deposition for *in situ* Fabrication of Tunnel Junctions. *Rev. Sci. Instrum.* **2014**, *85*, 073904.
(22) Lu, R.; Konzelmann, A.; Feng, X.; Gong, Y.; Liu, J.; Liu, Q.; Xin, M.; Hui, R.; Wu, J. High Sensitivity Surface Enhanced Raman Spectroscopy of R6G on *in situ* Fabricated Au Nanoparticle/Graphene Plasmonic Substrates. *Carbon* **2015**, *86*, 78−85.
(23) Xu, G.; Liu, J.; Wang, Q.; Hui, R.; Chen, Z.; Maroni, V. A.; Wu, J. Plasmonic Graphene Transparent Conductors. *Adv. Mater.* **2012**, *24*, OP71−76.

DOI: 10.1021/acsami.5b00336
ACS Appl. Mater. Interfaces 2015, 7, 8556−8561